American Journal of Nanoscience and Nanotechnology Research

American Journals of Nanoscience and Nanotechnology Research
http://www.ivyunion.org/index.php/ajnnr
Vol. 3, Article ID 201400552, 19 pages

Research Article

Effective Sidewall Functionalization of Multiwalled Carbon Nanotubes with Dichlorocarbene Addition using New Soluble Multi-site Phase Transfer Catalysts

G. Vimala* and E. Murugan

Department of Chemistry, Pachaiyappa's College for Women, India

Abstract

The novel soluble multi-site phase transfer catalysts (MPTCs), viz., 2,6-bis (triethylammoniummethylene chloride)-4-methoxytoluene (BTEACM) and 3,3',5,5'-tetrakis (dimethylaminopyridinium chloride) biphenyl (TDMAPCB) containing two, and four active sites was synthesized, and characterized through Fourier transform infra red spectroscopy (FTIR), proton nuclear magnetic spectroscopy, carbon nuclear magnetic spectroscopy, thermo gravimetric analysis (TGA) and energy dispersive spectroscopy (EDS) analyses. The obtained MPTCs were used as a catalysts for sidewall functionalization of multiwalled carbon nanotubes (MWCNTs) in dichlorocarbene (CCl_2) addition, and compared their functionalization yield with commercially available single site PTC and tri-site PTC viz., benzyltriethylammonium chloride (BTEAC) and 2,4,6-tris (triethylammoniummethylene chloride) mesitylene (TTEAMCM). The functionalization of CCl_2 on MWCNTs was established by the appearance of increased peak intensity of C-$Cl_{(str)}$ at 700 cm^{-1} and decreased peak intensity of C-$C_{(str)}$ at 1260 cm^{-1} in FTIR analysis. The increased I_D/I_G ratio from pristine MWCNTs (0.3) to MWCNT-CCl_2 hybrid (1.58) obtained from Raman studies strongly proved the covalent functionalization of CCl_2 on MWCNTs. Furthermore, the change of surface morphology, and increased diameter of MWCNT-CCl_2 hybrids obtained from irrespective of MPTCs were confirmed by scanning electron microscopy, high resolution transmission electron microscopy, and atomic force microscopy. Hence, TDMAPCB showed higher reactivity for sidewall functionalization of MWCNTs in CCl_2 addition.

Keywords: Multi-site phase transfer catalysts; Multi-walled carbon nanotubes; Scanning electron microscopy; High resolution transmission electron microscopy; Atomic force microscopy

Academic Editor: Taihong Shi, PhD, Department of Enviorment Science, Sun Yat-sen University, China

Received: October 26, 2014; **Accepted**: December 17, 2014; **Published**: January 20, 2015

***Correspondence to**: Dr. G. Vimala, Department of Chemistry, Pachaiyappa's College for Women, Kanchipuram – 631 501, Tamil Nadu, India; Email: vimalagopiin16@gmail.com

1. Introduction

The study of carbon nanotubes (CNTs) and its related nanomaterials are continuously growing since the landmark paper published by Iijima in 1991. In general, CNTs having excellent mechanical, electrical, and thermal properties due to their remarkable structure. They have potential applications in a variety of fields such as chemical,biological sensors, nanoelectronic devices, hydrogen storage, field emitters, catalyst supports, nanotube-reinforced materials, and supercapacitors [1,2]. To meet specific requirements demanded by particular applications, chemical functionalization of CNTs would be an important and essential step because that leads to increase both dispersibility and processability. CNTs are preferentially more reactive at the tube end caps with pentagonal defect sites than their sidewalls [3-6]. If it were possible to chemically modify the surface of the nanotube in a controlled manner, this would afford a number of opportunities for tailoring the structural and electronic properties [7]. There were some studies on the functionalization of CNTs with dichlorocarbene (CCl_2) and the theory of cycloaddition of dichlorocarbene was proposed usually with Seyferth reagents, such as, $ArHgCBr_2C1$and ArHgCBrCI [8-22]. Compare to single-walled carbon nanotubes (SWCN'l'), MWCNTs are much cheaper and can be functionalized for widespread use. Because, the halogen group is a good leaving group, which can be attacked by nucleophilic reagents, further modification may be carried out easily to dissolve the modified CNTs in solvents. Normally, cycloaddition of dichlorocarbene to olefins rather than benzene can be easily realized by reacting chloroform with a strong base.

Phase transfer catalysis is a versatile, well established synthetic tool applicable to a number of organic bi-phase reactions. This technique has become one of the most interesting and fascinating topics of research during the last few years since it being successful for a multitude of organic transformations [23-28]. Several soluble and insoluble forms of single-site phase transfer catalysts are already available commercially, but their utilities are limited owing to their low efficiency in the reactions. Particularly, some of the medically valuable products and intermediates were obtained only through high energy reaction conditions like high energy input or high concentration of catalyst, that too with low yield. Preference for phase transfer catalyst (PTC) arise from factors like low economy, high efficiency and low energy requirements. Hence, many studies are reported on attempts to develop multi-site phase transfer catalysts (MPTCs) containing more than one catalytic active site in a molecule. This is because, MPTCs offer the potential of providing greater PTC activity and accelerating the particular synthetic transformation even under mild conditions. Idoux *et al*. [29] were the first to synthesize MPTCs containing three phosphonium active sites in both soluble and insoluble polymer-supported forms. The catalytic activities of these MPTCs towards simple S_N^2 reaction and some weak nucleophile–electrophile S_NAr reactions were also reported. Balakrishnan and Ford [30] reported soluble ammonium PTCs containing two and three active sites. In our laboratory, we also reported different soluble and insoluble multi-site PTCs for alkylation reactions [31,32], dichlorocarbene addition [33], and asymmetric synthesis [34–38].

Very recently [39], we developed new MWCNT nanohybrids viz., MWCNT functionalized with amphiphilic poly(propyleneimine) (APPI) dendrimer carrying silver nanoparticles (AgNPs) and

demonstrated high dispersibility and antimicrobial activity. Subsequently to this report, we also developed an amphiphilic MWCNT polymer hybrid with improved conductivity and dispersibility produced by functionalization with Poly(vinylbenzyl)triethylammoniumchloride [40]. Further, we developed novel MWCNTs hybrid catalysts for effective catalysis of 4-nitrophenol reduction [41]. Few studies were already performed for sidewall functionalization of MWCNTs with dichloro, dibromo and difluro carbene addition reaction using soluble single-site PTCs. It is our impression that when the soluble single site PTC was used for functionalization of carbene on MWCNTs has directly depends on the activity of PTC. However, to the best of our knowledge, there is no report available on the functionalization of CCl_2 addition onto the MWCNTs using soluble MPTCs that too without much disrupting the electronic behavior of MWCNTs. Hence, in this study, we developed two types of new soluble multi-site phase transfer catalysts, viz., 2,6-bis(triethylammonium methylene chloride)-4-methoxytoluene (BTEACM) and 3,3',5,5'-tetrakis (dimethylamino pyridinium chloride) biphenyl (TDMAPCB) having two and four active sites respectively through simplified procedures with inexpensive starting materials. Further, the catalytic activity of these newly developed MPTCs and commercial single-site and tri-site PTCs such as benzyltriethylammonium chloride (BTEAC), and 2,4,6-tris (triethylammonium methylene chloride) mesitylene (TTEAMCM) respectively were inspected through sidewall functionalization of dichlorocarbene on MWCNTs through addition reaction keeping under identical experimental condition. The obtained MWCNTs-CCl_2 yield from each catalyst was compared with the yield obtained through catalysis of known soluble PTCs such as BTEAC, and TTEAMCM catalysts performed under same experimental condition. Similarly, the yields of MWCNTs hybrids viz., MWCNTs-CCl_2-1 (single-site), MWCNTs-CCl_2-2 (di-site), MWCNTs-CCl_2-3 (tri-site), and MWCNTs-CCl_2-4 (tetra-site) were thoroughly characterized with spectral, thermal and microscopic techniques and based on the spectral results the effective MPTC for CCl_2 functionalization of MWCNTs was identified.

2. Experimental section

2.1. Materials

MWCNT with purity higher than 95% was obtained from Sigma-Aldrich. 4-methoxytoluene (SRL), formaldehyde (SRL), calcium oxide (CaO, Merck), dichloromethane (DCM, Merck), thionyl chloride ($SOCl_2$, Merck), acetonitrile (CH_3CN, SRL), triethylamine (Et_3N, Merck), sodium chloride (NaCl, Merck), zinc chloride ($ZnCl_2$, SRL), ethanol (C_2H_5OH, Merck), 3,3',5,5'-tetramethylbiphenyl (Aldrich), paraformaldehyde (Lancaster), Con. hydrochloric acid (Con.HCl, Merck), dimethylaminopyridine (DMAP, SRL), chloroform ($CHCl_3$, SRL), sodium hydroxide (NaOH, SRL) were analar grade and used as received.

2.2. Characterization

Fourier transform infrared (FTIR) spectra were recorded on a Bruker Tensor-27 FTIR spectrophotometer

with OPUS software and the sample for analysis was prepared by taking equal amounts of each sample and KBr (1:1 ratio) and the corresponding pellet was carefully prepared with uniform thickness. The ^{1}H NMR and ^{13}C NMR spectra were recorded using JEOL 400 MHz and Bruker ARX 200 MHz spectrometers respectively. The thermogravimetric analysis (TGA) was carried out on SDT Q600 V20.5 Build 15 instrument at a heating rate of 10^{o}C/min from 50 to 800 ^{o}C under nitrogen atmosphere. Raman spectra were acquired with a Witec Confocal Raman instrument (CRM200) with Ar ion laser (514.5 nm). Scanning electron microscopy (SEM) measurements were carried out on a HITACHI S-3000H scanning electron microscope with an accelerating voltage of 2 kV. The sample for analysis was prepared by taking equal amounts and spreading on the surface of double-sided adhesive tape, one side was already adhered to the surface of a circular copper disc pivoted by a rod and the spreaded samples were sputtered with gold prior to SEM observation. Energy dispersive spectroscopy (EDS) was performed on EDS DX–4 energy diffraction spectrometer of the SEM and the observed percentage of elements was compared quantitatively. High resolution transmission electron microscopy (HRTEM) analysis was carried out on JEOL 3010 transmission electron microscope instrument operating at 200 kV. The sample to be analyzed was sonicated with ethanol for few minutes and then one drop of each sample (suspension) was placed on a glow discharged carbon- coated grid followed by the evaporation of the solvent for the HRTEM observation. AFM samples were prepared by coating a mica surface with a drop of MWCNTs hybrids dispersed in ethanol. AFM tests were carried out in "tapping" mode under ambient conditions using a single beam cantilever (225 μm length) provided by an etched silicon nitride probe having a tip of nominal radius of curvature of 5–10 nm, at a scan rate of 1 line/s. Topographic images of the individual MWCNT hybrids were recorded by Agilent technologies digital instrument.

2.3. Preparation of di-site and tetra-site MPTCs

2.3.1. Preparation of BTEACM (Scheme 1)

In a 250 ml single-necked RB flask, 6.2 g (50 mmol) of 4-methoxytoluene **(1)** was dissolved in 40 ml water and 9.2 ml of formaldehyde solution (37 %) were added to it. To this mixture, 1.6 g (28.5 mmol) of calcium oxide was added and stirred for 24 hrs. The resulting mixture was treated with 4 ml of acetic acid and the container was kept in freezing mixture at 0^{o}C till the solution yielded white colored crystals. The resulting solid product was recrystallized using hexane. The melting point of the product is 128^{o}C, yield 55 %. In the second step, 2,6-bis(hydroxymethyl)-4-methoxytoluene **(2)** (5 g, 27 mmol) was dissolved in dry dichloromethane (20 ml) and transferred into a 100ml RB flask. To this solution, 20 ml of thionyl chloride was added slowly and the mixture was refluxed for 12 hrs in nitrogen atmosphere. The resulting yellow solid was washed with DCM and dried under vacuum to yield the chlorinated product viz., 2,6-bis(chloromethyl)-4-methoxytoluene **(3)**. The yield was 83 % and mp. 105^{o}C. Finally, the 2,6-bis (chloromethyl)-4-methoxytoluene **(3)** 5 g (22.6 mol) (3) was dissolved in dry acetonitrile (30 ml) and transferred into a 100 ml RB flask. The solution was deaerated and triethylamine (40 ml) was added to the solution. The reaction mixture was gently refluxed for 24 hrs under nitrogen atmosphere and thus a

white precipitate of quaternized product of di-site PTC, BTEACM **(4)** was obtained. The resulting product was recrystallized using ethanol. Yield 90 %, melting point was 190^{o}C.

FT-IR (KBr, cm^{-1}) : 3434 (O-H), 2940 (C-H), 702 (C-Cl), and 1154 (C-N) (Figure 1b).

^{1}H NMR (300 MHz, $CDCl_3$) δ: 1.43-1.48 (t, 18H, methyl), 3.15-3.24 (q, 12H, methylene), 4.67 (s, 4H, methylene).

^{13}C NMR (75 MHz, $CDCl_3$) δ: 8.6, 20.8, 45.9, 60.9, 62.2, 129.5, 134.3, 153.9.

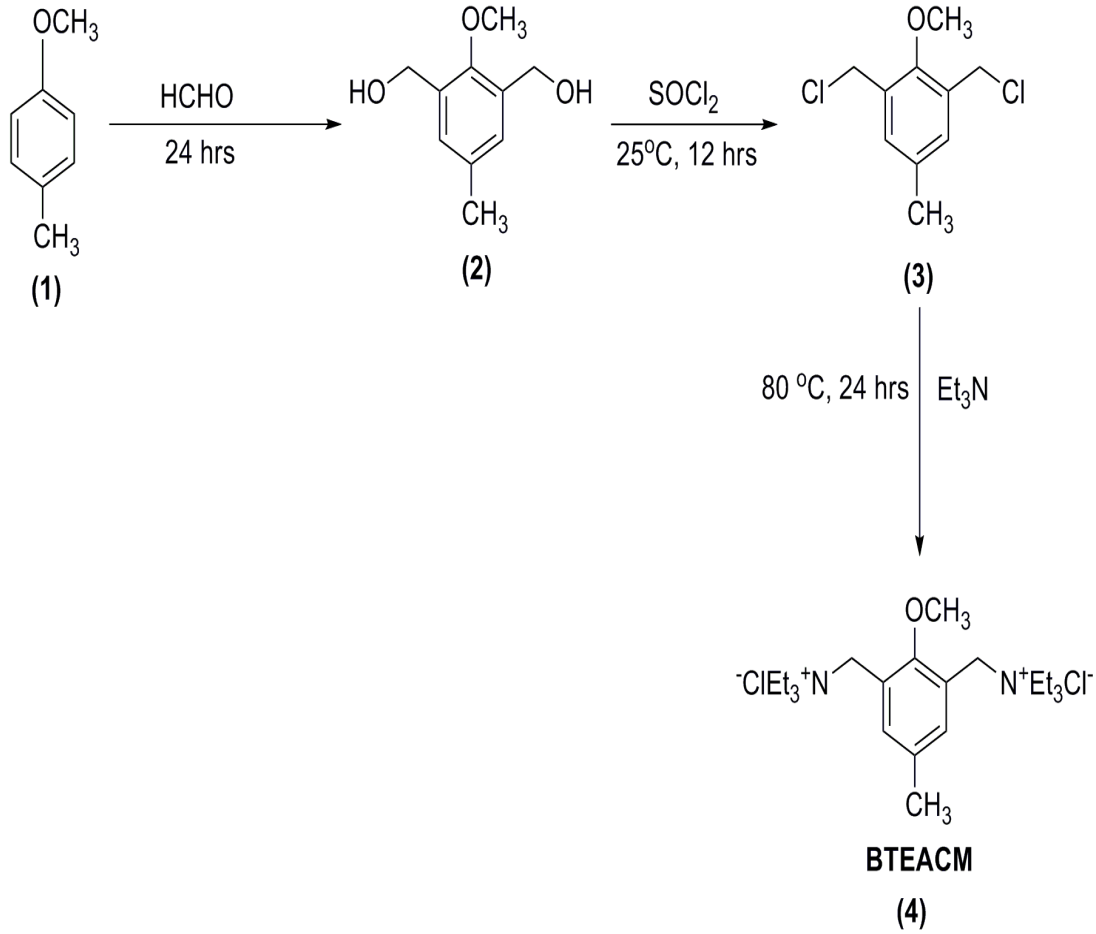

Scheme 1 Synthesis of Di-site PTC

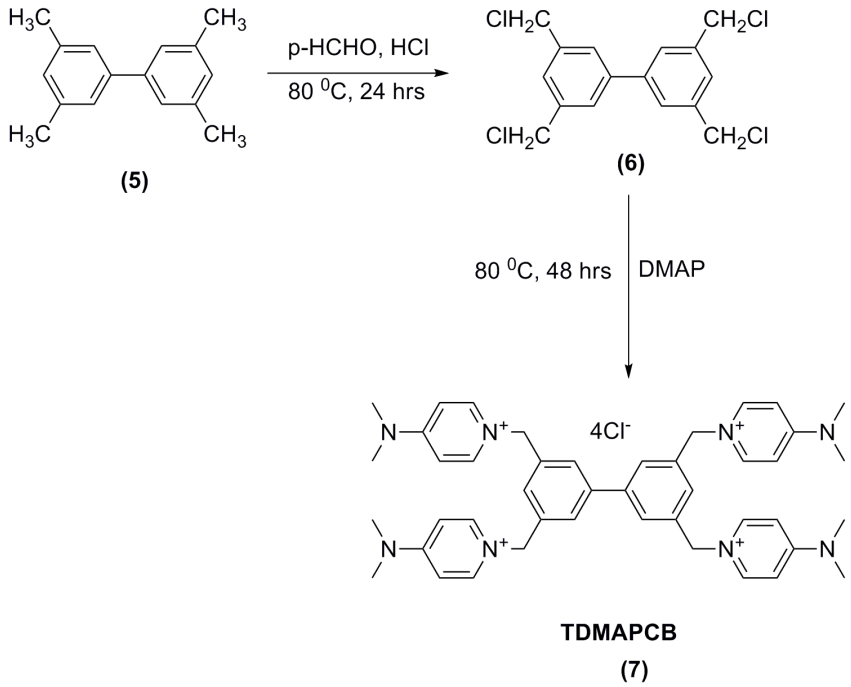

Scheme 2 Synthesis of tetra-site PTC

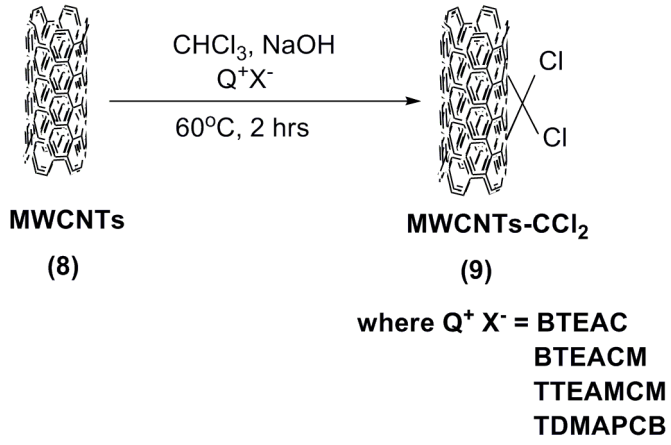

Scheme 3 Sidewall functionalization of MWCNTs for dichlorocarbene addition using MPTCs

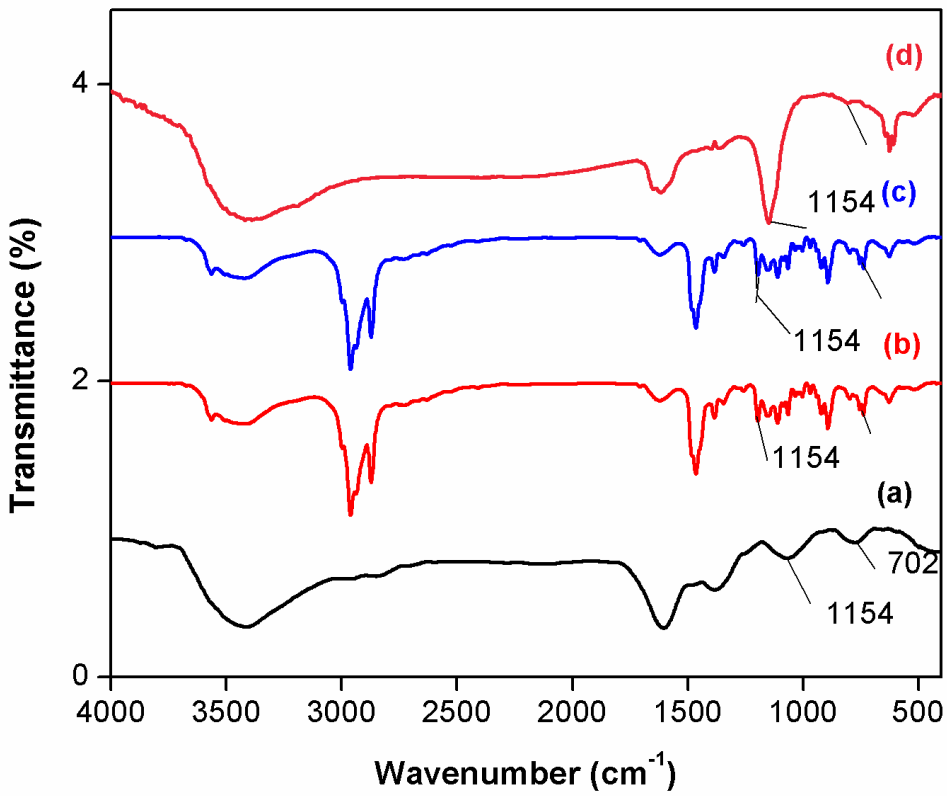

Figure 1 FTIR Spectra of (a) BTEAC, (b) BTEACM, (c) TTEAMCM and (d) TDMAPCB

2.3.2. Preparation of TDMAPCB (Scheme 2)

In a 150 ml RB flask, tetramethylbiphenyl **(5)** (2 g, 1.96 mmol) was dissolved in 15 ml of Con.HCl and the reaction mixture was stirred. Then, paraformaldehyde (3.6 g, 120 mmol) and zinc chloride (4 g, 30 mmol) were added into the above mixture and refluxed gently at 80°C for 24 hrs. The resulting product 3,3',5,5'-tetrakis(chloromethyl) biphenyl **(6)** was recrystallized using hexane. Yield 86 %, melting point 103-104 ^{o}C. In the second step, the product **(6)** (2 g, 3.63 mmol) was dissolved in 30 ml of acetonitrile and 25 ml of dimethylaminopyridine was added in 100 ml RB flask. The reaction mixture was refluxed at 80^{o}C for 12 hrs in a N_2 atmosphere. Then the resulting product TDMAPCB **(7)** was recrystallized from ethanol. The melting point of the product is 190^{o}C, yield 86 %.

FT-IR (KBr, cm^{-1}): 1154 (C-N) (Figure 1d).

^{1}H NMR (300 MHz, $CDCl_3$) δ: 2.05 (s, 8H, methylene), 8.2, (d, aromatic), 6.96 (d, aromatic).

^{13}C NMR (75 MHz, $CDCl_3$) δ: 40.4, 106.7, 122.5, 124.8, 131.9, 134.2, 142.7, 155.6.

2.4. Catalysis of soluble single and MPTCs for sidewall functionalization of dichlorocarbene on MWCNTs

200 mg of pristine MWCNTs **(8)** and 15 ml of chloroform were taken in four different 100 ml round bottomed flask and the mixture was dispersed in ultrasonicator for 15 min. Then, 1.186 x 10^{-4} mole of BTEAC, BTEACM, TTEAMCM, and TDMAPCB were added to the respective containers and the resulting solutions were ultrasonicated for 30 min. Subsequently, 10 ml of sodium hydroxide solution was

added to each container and then refluxed for about 2 hrs. The reaction mixtures were cooled to room temperature, and poured into 15 ml water and again sonicated for 10 min. The resulting mixture containing MWCNTs functionalized with dichlorocarbene products were washed, centrifuged and thus black color powder was obtained. The black powder derived from each catalyst was dried in vacuum at 120^{o}C and weighed (0.356 g of MWCNTs-CCl_2-1, 0.478 g of MWCNTs-CCl_2-2, 0.624 g of MWCNTs-CCl_2-3 and 0.891 g for MWCNTs-CCl_2-4 **(9) (**Scheme 3).

3. Results and discussion

Characterization of BTEACM and TDMAPCB

3.1. FTIR, H^1NMR and C^{13}NMR

Two different new soluble MPTCs including BTEACM (di-site) and TDMAPCB (tetra-site) were prepared by adopting the simplified procedures. The availability of number of quaternary ammonium groups (catalytic-site) in each catalyst was established with FTIR, ^{1}H NMR, ^{13}C NMR, TGA and EDS analyses. The structure of di-site and tetra-site MPTCs were confirmed by the disappearance of C-Cl stretching at 700 cm^{-1} and appearance of C-N stretching at 1154 cm^{-1} in respective FTIR spectrum. However, the number of quaternary onium group present in each catalyst was estimated semi-quantitatively through comparative FTIR study. The comparative FTIR results reveals that the C-N peak intensity noticed at 1154 cm^{-1} has been gradually increased from BTEAC (single-site) to TDMAPCB (tetra-site) and this in turn proves the linear increase of number of quaternary onium groups in BTEACM (di-site) and in TDMAPCB (tetra-site) catalysts (Figure 1).

In the ^{1}H NMR analysis, the quarternized ethyl group consisting of methyl and methylene protons showed triplet and quartet at 1.43-1.48 and 3.15-3.24 ppm, respectively for di-site and the methyl protons (8 Nos.) of DMAP gave a singlet at 2.05 ppm, the characteristic peak viz., pyridine ring protons appeared as a doublet at 7.3 and 8.2 ppm; the biphenyl ring protons showed a doublet at 6.62 and 6.96 ppm for tetra-site and thus supporting the formation of quaternizing groups. Similarly, in ^{13}C NMR, the methyl and methylene carbon showed strong intense peak at 8.6 and 45.6 ppm respectively for di-site and the methyl carbons of DMAP was observed at 40.4 ppm, the aromatic carbons of pyridine ring showed signals at 106.7, 142.7 and 155.6 ppm, and the biphenyl ring carbons showed signal at 122.5, 124.8, 131.9 and 134.2 ppm for tetra site, thus strongly supported the formation of quaternizing sites. Wang *et al*.[42] synthesized a di-site PTC by quaternization of α,α'-dichloro-*p*-xylene with triethylamine in ethanol medium and its structure was established through FT-IR and NMR analyses. Vajjiravel et al. [43] synthesized a di-site PTC viz., 1,4-bis (tributylmethylammonium chloride) benzene by quaternizing 1,1-dichloro-*p*-xylene and tributylamine.

3.2. TGA and EDS analysis

The presence of more active sites in MPTCs was further verified through TGA. The amount of catalytic functional groups –$N(C_2H_5)_3$, present in each catalyst was ascertained from its percentage of weight loss which in turn revealed the number of active sites quantitatively. Irrespective of the MPTCs, decomposition of triethylamine group was noticed in the range of 160-300^{o}C and Wu and Lee was also reported same

temperature range [44]. The observed weight loss of $–N(C_2H_5)_3$ group for single site PTC was 1.02%, for di-site PTC 2.75%, for tri-site PTC 3.42%, and for tetra site PTC 4.59% (Table 1). The percentage of weight loss was gradually increased from single-site to tetra site PTC. The percentage of weight loss of $–N(C_2H_5)_3$ group was a direct quantitative measure for availability of number of active sites, the higher weight loss of $–N(C_2H_5)_3$ was observed for tetra site PTC, and lower weight loss value observed for single site PTC. It provided a quantitative measure of active sites in respective catalysts.

Table 1 Comparative TGA and EDS results of soluble single site PTC and MPTC's.

S.No	Name of MPTCs	TGA (% Yield)	EDS (wt %) C	N	Cl
1.	BTEAC (single-site)	1.02	52.1	5.07	10.46
2.	BTEACM (di site)	2.75	54.6	6.87	14.89

Similarly, the EDS analysis is one of the most effective characterization techniques for identification and quantification (semi-quantitative) of the elements present in single site, di-site, tri-site and tetra site MPTCs. From the EDS results (Table 1), it was observed that the percentage of carbon, nitrogen and chloride increased with an increase in number of active sites from single site PTC to tetra site PTC. This observation additionally confirmed the availability of multi active sites present in the respective MPTCs.

3.3. Sidewall Functionalization of MWCNTs with dichlorocarbene addition using soluble MPTCs

3.3.1. FTIR Study

The FTIR spectra derived from MWCNTs-CCl_2 hybrids obtained each catalyst viz., BTEAC, BTEACM, TTEAMCM, and TDMAPCB are shown in Figure 2 a-d respectively. The appearance of peaks for C-$C_{(str)}$ and C-$Cl_{(str)}$ at 1260 cm^{-1} and 700 cm^{-1}, respectively, confirmed the functionalization of CCl_2 on MWCNTs. Since, the FTIR spectra of all the MWCNTs-CCl_2 hybrids were recorded by semi-quantitative mode, the peak intensity of the characteristic peaks was taken to be proportional to the amount of CCl_2 functionalized on each MWCNTs hybrid. Further, it was also seen that the peak intensity of C-$Cl_{(str)}$ at 700 cm^{-1} gradually increased from MWCNTs-CCl_2 hybrids obtained from single-site PTC (BTEAC) to tetra-site MPTC (TDMAPCB) and on the contrary, the peak intensity of C-$C_{(str)}$ decreased from product of MWCNTs-CCl_2 derived from single-site PTC to tetra-site MPTC. This trend indicated the amount of CCl_2 functionalized on the respective MWCNTs hybrid. The amount of CCl_2 functionalized on MWCNTs was in the order single site > di-site > tri-site > tetra site PTC, and this order in turn reflected the activity of the each catalyst (or) presence of number of quaternary onium groups in each catalyst. Normally, the peak intensity was directly related to the quantum of functionalized yield [45], hence it supported our observation.

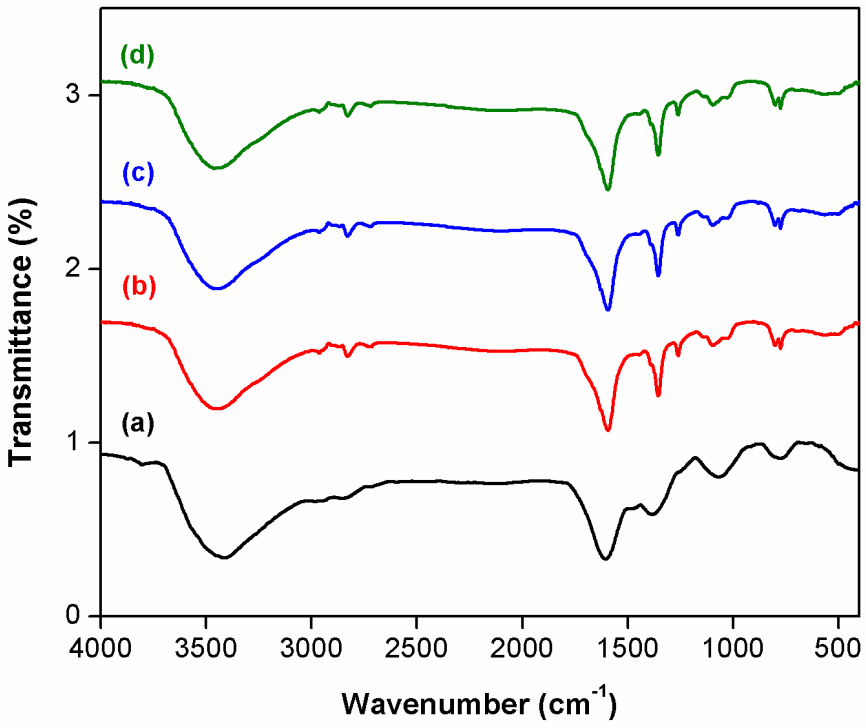

Figure 2 FTIR spectra of (a) MWCNTs-CCl_2-1, (b) MWCNTs-CCl_2-2, (c) MWCNTs-CCl_2-3, and (d) MWCNTs-CCl_2-4.

3.3.2. Raman Spectral Study

The Raman spectra of MWCNTs-CCl_2 functional hybrids derived from catalysis of single site, di-site, tri-site and tetra-site were recorded under 514.5 nm excitation over the Raman shift interval of 1000 - 3000 cm^{-1} and they are shown in Figure 3. Normally, the defect/disorder in MWCNT can be established through appearance of the two distinct absorption bands at 1330 cm^{-1} (D band) and 1580 cm^{-1} (G band). They are assigned to the vibration of sp^2-bonded carbon atoms in the planar hexagonal graphite lattice. It is generally known that the D to G-band intensity ratio (I_D/I_G) is an approximate indication for the degree of defects/disorder in pristine MWCNTs due to functionalization [46-48]. The observed I_D/I_G ratio for 4 types of MWCNTs-CCl_2 hybrids along with pristine MWCNTs are given in Table 2. The I_D/I_G ratio of pristine MWCNTs is 0.3 which was increased depending on the amount of CCl_2 functionalization on MWCNTs. The I_D/I_G ratio for MWCNTs-CCl_2 hybrid derived from single-site PTC was 1.2, for di-site PTC catalyzed hybrids 1.36, for tri-site 1.42 and for tetra-site PTC was 1.58. The gradual increase of I_D/I_G ratio for MWCNTs-CCl_2 hybrids derived from catalysis of single-site PTCs to MWCNTs-CCl_2 hybrids derived from tetra-site MPTC proved the proportionate sidewall functionalization of CCl_2 onto the respective MWCNTs. To highlight briefly, based on the number of active sites present in the PTC, the degree of sidewall functionalization of CCl_2 in MWCNTs is varied. The I_D/I_G values revealed that on increasing the active site the covalent functionalization yield of CCl_2 has also increased parallely and thus reflected increased I_D/I_G values.

Table 2 Comparative Results of Dichlorocarbene Functionalized MWCNTs using Different Soluble MPTC's.

S.No	Name of the MWCNTs hybrids	I_D/I_G [a]	Yield, % [b]	EDS (wt %)		HRTEM [c]	AFM [d]
				C	Cl	nm	nm
1.	Pristine MWCNTs	0.3	-	99.99	-	120	120
2.	MWCNTs-CCl_2-1	1.2	0.9	61.95	16.37	136	147
3.	MWCNTs-CCl_2- 2	1.36	1.06	53.83	24.08	150	155
4.	MWCNTs-CCl_2- 3	1.42	3.38	48.14	31.79	168	170
5.	MWCNTs-CCl_2- 4	1.58	12	39.17	41.09	190	197

[a] - determined by Raman analysis
[b] - percentage yield determined by TGA analysis
[c] - diameter of the MWCNTs-CCl_2 hybrids determined by HRTEM analysis
[d] - diameter of the MWCNTs-CCl_2 hybrids determined by AFM analysis

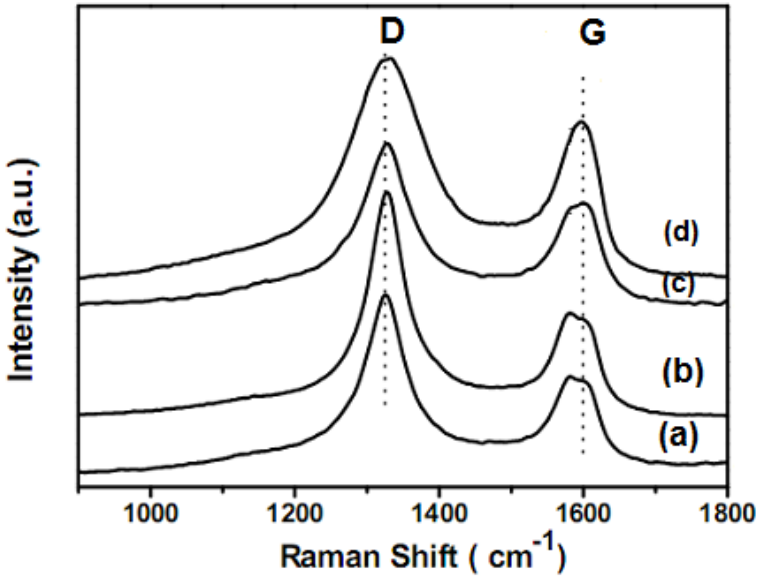

Figure 3 Raman spectra of (a) MWCNTs-CCl_2-1, (b) MWCNTs-CCl_2-2, (c) MWCNTs-CCl_2-3, and (d) MWCNTs-CCl_2-4.

3.3.3. TGA analysis

TGA was performed for all the MWCNTs-CCl_2 hybrids derived from each catalyst and determined the quantitative of CCl_2 molecules functionalized onto the MWCNTs, and the results are presented in Table 2.

The thermograms derived from dichlorocarbene functionalized four different MWCNTs-CCl_2 hybrids obtained from 4 different catalysts are shown in Figure 4 a-e. The thermogram of pristine MWCNTs is shown in Figure 4a. The percentage of weight loss in the MWCNTs-CCl_2-1 hybrid to MWCNTs-CCl_2-4 hybrid obtained from catalysis of single-site, di-site, tri-site PTC and tetra-site PTC are given in Table 2. The pristine MWCNTs did not show any weight loss even upto 800^{o}C. In contrast, the other 4 types of MWCNTs-CCl_2 hybrids were showed different ranges of weight loss between 200 to 450^{o}C. The percentage of weight loss for MWCNTs-CCl_2-1 hybrids was 0.9 % (Figure 4b), for di-site catalyzed hybrid viz., MWCNTs-CCl_2-2 1.06 % (Figure 4c), for MWCNTs-CCl_2-3 3.38 % (Figure 4d), and for MWCNTs-CCl_2-4 12% (Figure 4e). These results showed that the degree of CCl_2 loss has been gradually increased from MWCNTs-CCl_2-1 hybrids to MWCNTs-CCl_2-4 hybrids. Alternatively, the degree of CCl_2 functionalized yield derived from MWCNTs-CCl_2-1 to MWCNTs-CCl_2-4 hybrids enhanced due to the impact of the activity of the corresponding soluble MPTC. The single-site PTC (BTEAC) produced less percentage of CCl_2 loss in MWCNTs-CCl_2-1 than the corresponding higher numbered MPTCs. Otherwise, the tetra site PTC showed two fold weight loss compared to the corresponding di-site PTC (BTEACM) suggesting higher degree of dichlorocarbene functionalization in MWCNTs-CCl_2-4 compared to MWCNTs-CCl_2-2 hybrids, and thus provided lower percentage of weight loss. Hence, the degree of percentage weight loss was proportional to the extent of sidewall functionalization of CCl_2 attached on MWCNTs, and this in turn correlated to the number of catalytic sites present in each PTC.

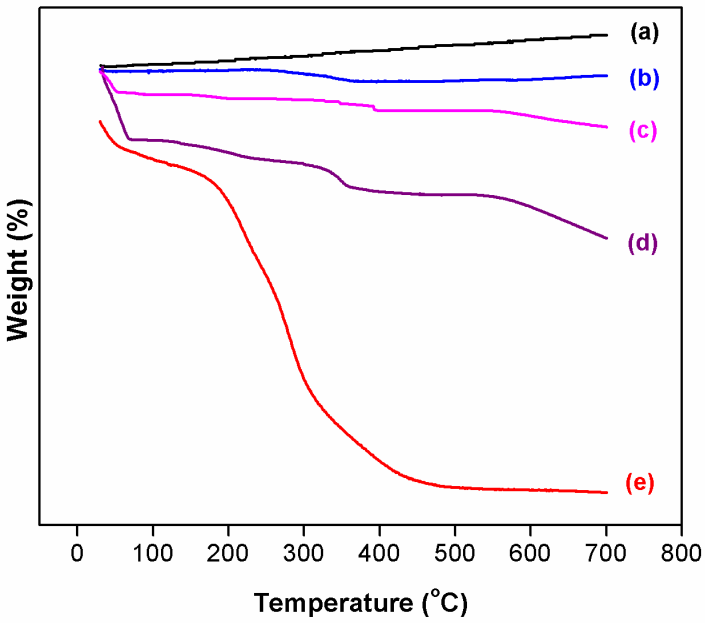

Figure 4 TGA curves of (a) pristine MWCNTs, (b) MWCNTs-CCl_2-1, (c) MWCNTs-CCl_2-2, (d) MWCNTs-CCl_2-3, and (e) MWCNTs-CCl_2-4.

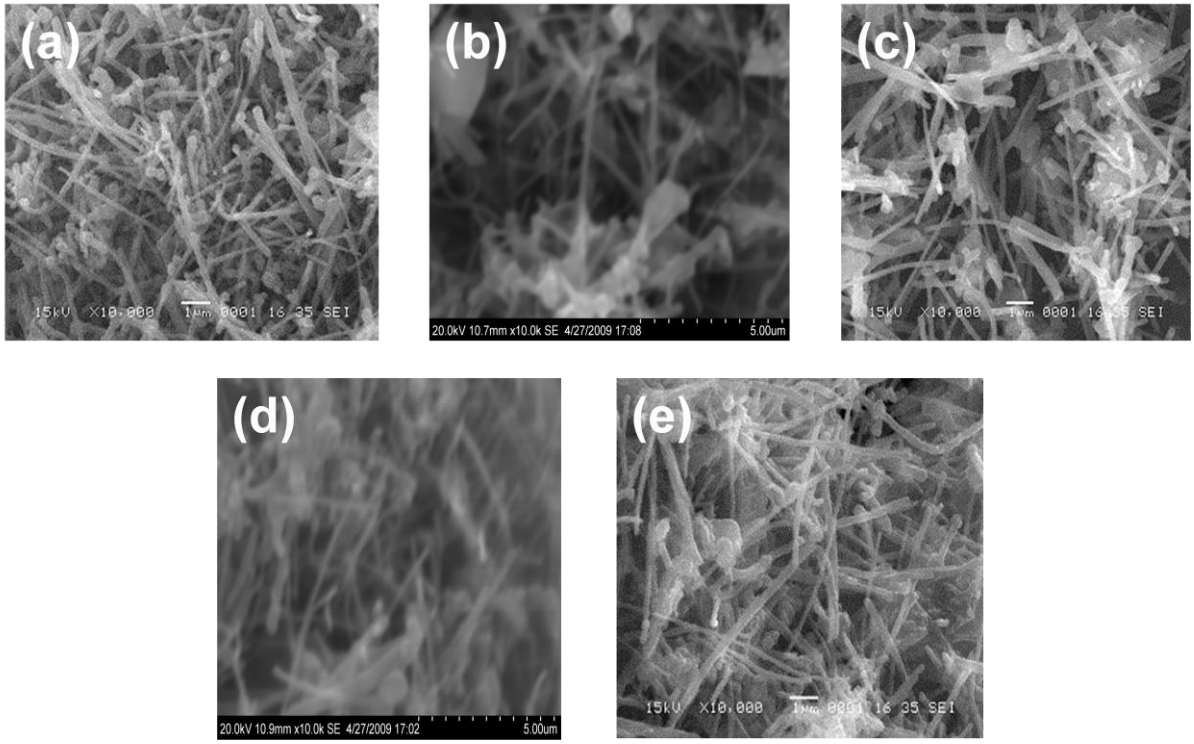

Figure 5 SEM images of (a) pristine MWCNTs, (b) MWCNTs-CCl_2-1, (c) MWCNTs-CCl_2-2, (d) MWCNTs-CCl_2-3, and (e) MWCNTs-CCl_2- 4.

3.3.4. SEM & EDS

The variation of surface morphology of MWCNTs due to sidewall functionalization of CCl_2 was ascertained from the SEM images recorded for pristine MWCNTs and all the other 4 hybrids viz., MWCNTs-CCl_2-1, MWCNTs-CCl_2-2, MWCNTs-CCl_2-3 and MWCNTs-CCl_2-4. The recorded SEM images are shown in Figure 5a-e. Based on the intensity of CCl_2 functionalization on MWCNTs, the smooth surface of the pristine MWCNTs (Figure 5a) became rough and heterogeneous as observed in Figure 5b-e. The MWCNTs-CCl_2-1 hybrid derived from catalysis of single-site PTC contained less coverage of white patches and less heterogeneity than the images of MWCNTs-CCl_2-2. The image of MWCNTs-CCl_2-3 showed relatively better coverage of white patches, rough surface and debundled SWCNT compared to MWCNTs-CCl_2-2 hybrid. Especially, the images recorded from MWCNTs-CCl_2-4 derived by functionalization with CCl_2 due to catalysis of tetra site PTC showed more white coverage, debundled SWCNT and heterogeneous surface. Therefore, the variation of smooth surface morphology of pristine MWCNTs to heterogeneous surface with white coverage and appearance of debundled SWCNT confirmed sidewall functionalization of MWCNTs with CCl_2. The intensity of the white coverage, heterogeneous surface and debundled SWCNT were directly related to degree of the amount of CCl_2 functionalization, and its content was a measure for the catalytic potential of each PTCs. Since, the intensity/heterogeneous surface/appearance of debundled SWCNT increased from MWCNTs-CCl_2-1 to MWCNTs-CCl_2-4 hybrid, the catalytic potential and presence of number of catalytic sites in the respective catalysts were also proved beyond doubt.

The quantum of covalent functionalization of CCl_2 on all the four hybrids was investigated semi-quantitatively with EDS. The EDS spectra of pristine MWCNTs and 4 types of each MWCNTs hybrid are shown in Figure 6a-e, and the weight percentage of carbon and chlorine determined from each spectrum are given in Table 2. The spectrum for pristine MWCNTs showed only carbon peak (Figure 6a)

with 99.99%, whereas, the spectra of MWCNTs-CCl_2-1 to MWCNTs-CCl_2-4 indicated that the peak intensity of carbon consistently decreased and that of chloride increased proportionately. The peak due to Na was seen in all the EDS of four MWCNTs hybrids, and the appearance of this sodium peak was due to the use of NaOH and $CHCl_3$ for CCl_2 generation. The percentage of carbon and chloride (Table 2) suggested that percentage of carbon for MWCNTs-CCl_2-1 to MWCNTs-CCl_2-4 hybrids decreased from 61.95 to 39.17 %, but in contrast the chloride percentage increased from 16.37 to 41.09%. The decreased percentage of carbon with increased percentage of chloride provided strong evidence for periodical increase of covalent functionalization of CCl_2 for MWCNTs-CCl_2-1 to MWCNTs-CCl_2-4 hybrids. Hence, the single site PTC helped for lower sidewall functionalization of CCl_2, whereas, the di-site, tri site and tetra site PTCs performed in proportion to the availability of active sites.

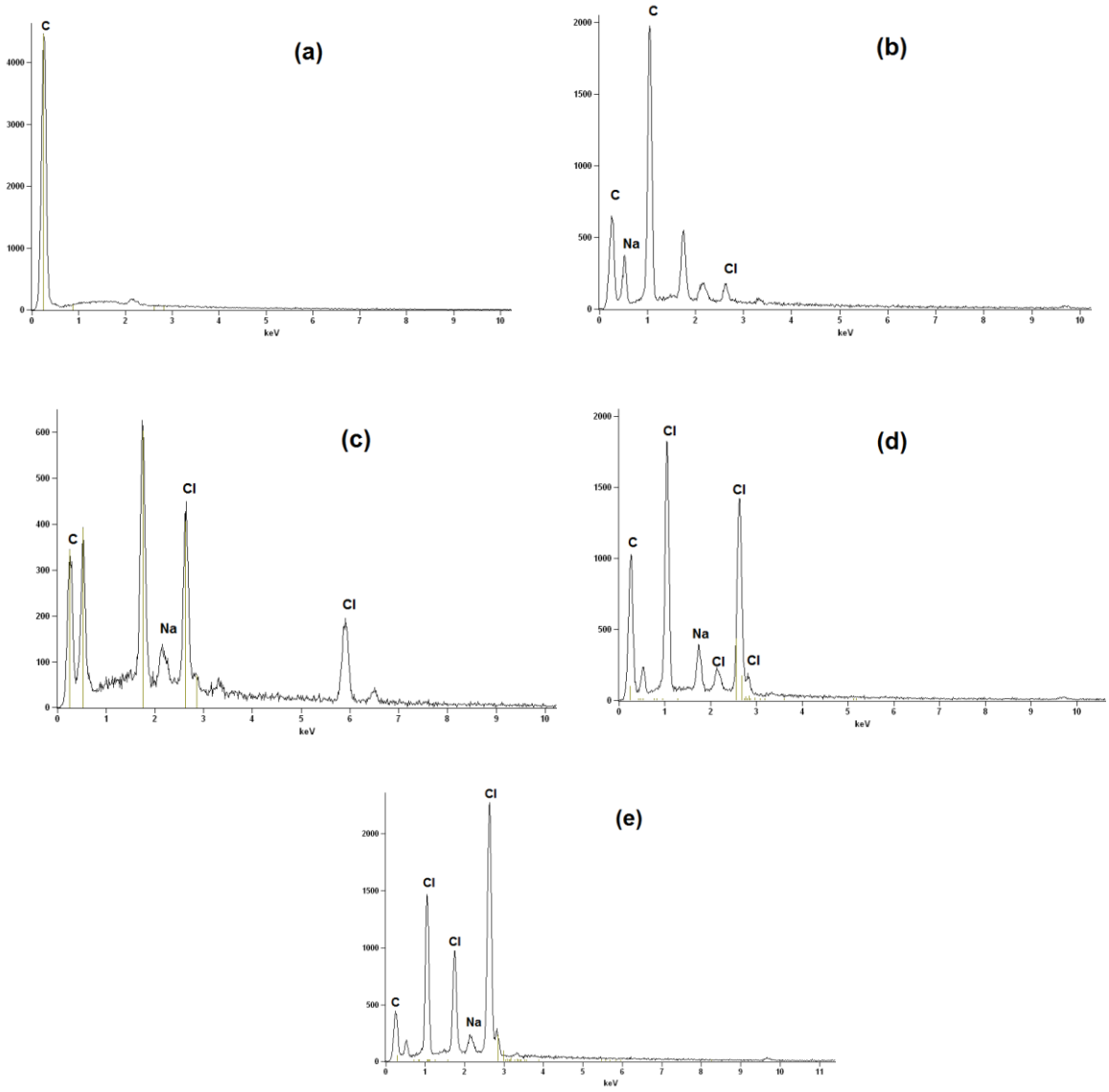

Figure 6 EDS spectra of (a) pristine MWCNTs, (b) MWCNTs-CCl_2-1, (c) MWCNTs-CCl_2-2, (d) MWCNTs-CCl_2-3, and (e) MWCNTs-CCl_2- 4.

3.3.5. HRTEM

The change of surface morphology of MWCNTs hybrids derived from catalysis of single-site PTC to tetra-site PTC viz., MWCNTs-CCl_2-1, MWCNTs-CCl_2-2, MWCNTs-CCl_2-3, and MWCNTs-CCl_2-4 through HRTEM and the images for pristine MWCNTs and 4 MWCNTs-CCl_2 hybrids are shown in Figure 7 a-e. The observations derived from SEM images were once again confirmed by HRTEM results. Depending on the amount of sidewall functionalization of CCl_2, the smooth surface of the pristine MWCNTs became rough/heterogeneous in nature. Further, here too, the heterogeneously distributed white coverage and debundled SWCNT due to CCl_2 functionalization were observed. Particularly, the images recorded from MWCNTs-CCl_2-1 to MWCNTs-CCl_2-4 produced more isolated SWCNT with increased variable wall thickness of white coverage. The intensity of white coverage onto the isolated/debundled SWCNT was a direct measure of increased functionalization of CCl_2. Since the tetra site PTC, TDMAPCB, was able to produce more CCl_2 from $CHCl_3$/NaOH, and functionalize on MWCNTs, it led to debundled and isolated SWCNT/tubes with thick white coverage. Similarly, other PTCs viz., BTEAC (single-site), BTEACM (disite) and TTEAMCM (trisite) PTC also produced CCl_2 relative to their catalytic sites, functionalized MWCNTs, and appeared as a white coverage. More importantly, based on the quantum of CCl_2 functionalized onto the MWCNTs, the diameter of the resulting MWCNTs hybrids varied (Table 2). The measured diameter of the MWCNTs hybrids derived from MWCNTs-CCl_2-1, MWCNTs-CCl_2-2, MWCNTs-CCl_2-3 and MWCNTs-CCl_2-4 was 136, 150, 168 and 198 nm, respectively. Thus, the increased diameter of the MWCNTs-CCl_2 hybrids was due to intense functionalization of CCl_2 and so also the catalytic activity of the corresponding PTCs.

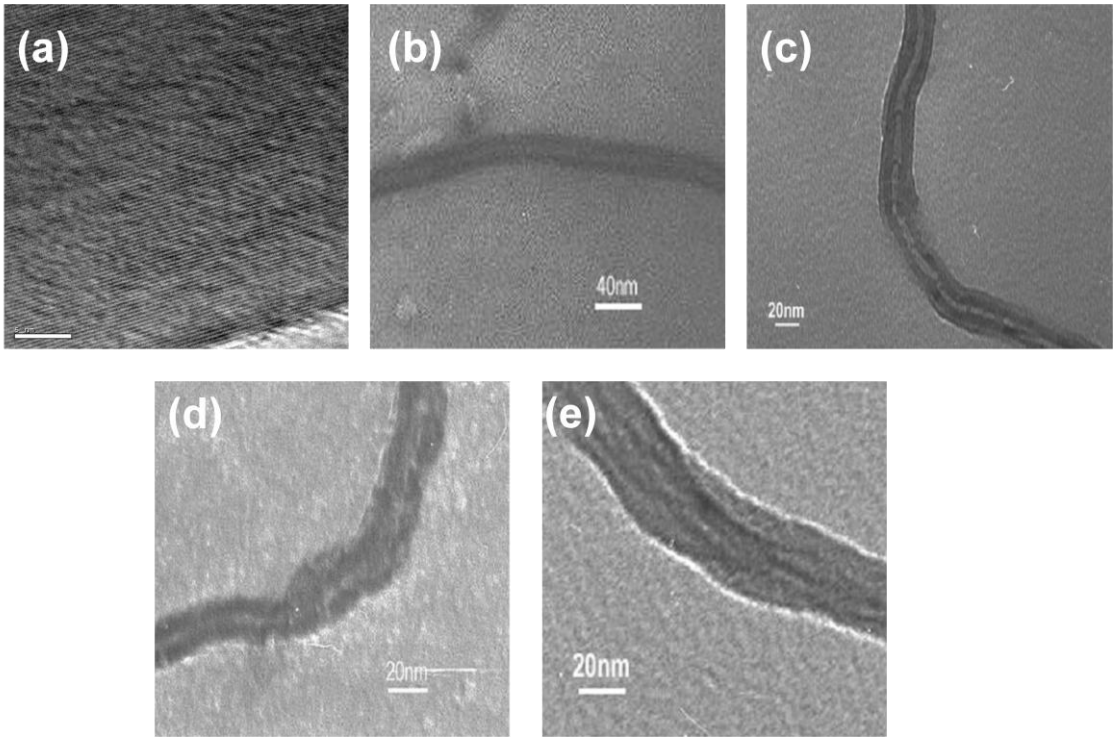

Figure 7 HRTEM images of (a) pristine MWCNTs, (b) MWCNTs-CCl_2-1, (c) MWCNTs-CCl_2-2, (d) MWCNTs-CCl_2-3, and (e) MWCNTs-CCl_2- 4.

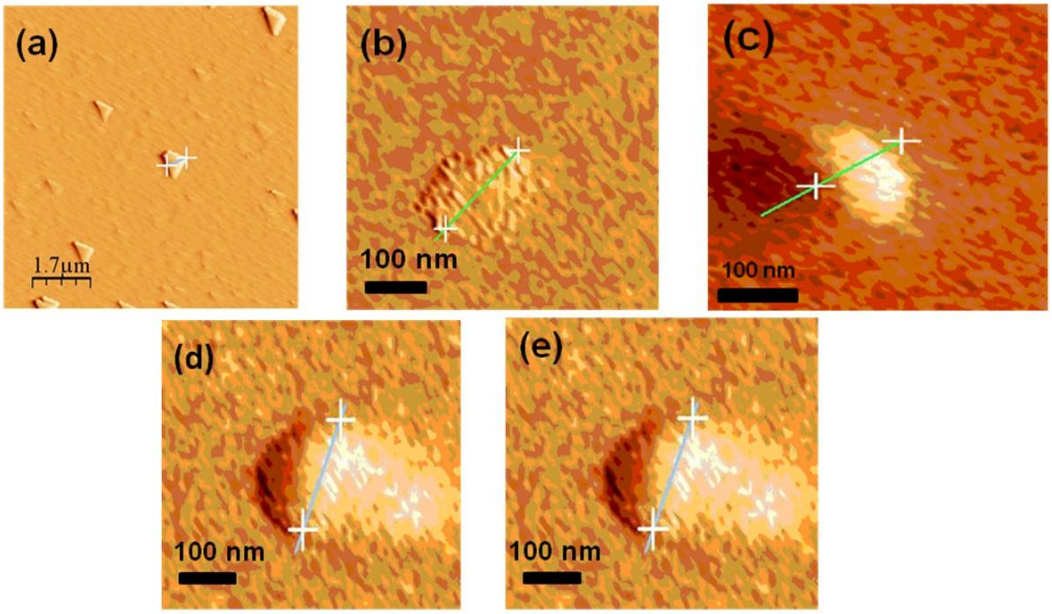

Figure 8 AFM images of (a) pristine MWCNTs, (b) MWCNTs-CCl_2-1, (c) MWCNTs-CCl_2-2, (d) MWCNTs-CCl_2-3, and (e) MWCNTs-CCl_2- 4.

3.3.6. AFM

The functionalization of CCl_2 on MWCNTs in all the 4 hybrids was further characterized by AFM analysis and the recorded images for pristine MWCNTs and 4 MWCNTs-CCl_2 hybrids are shown in Figure 8 a-e. The pristine MWCNTs aggregated into large bundles of several micrometers in length and several tens to a hundred nanometers in diameter (Figure 8a). In contrast, the AFM image of the 4 types of MWCNTs-CCl_2 hybrids showed exfoliated MWCNTs and increased white coverage with diameter of 147 nm for MWCNTs-CCl_2-1, 155 nm for MWCNTs-CCl_2-2, 170 nm for MWCNTs-CCl_2-3, and 197 nm for MWCNTs-CCl_2-4. On comparing, the diameter of the 4 types of MWCNTs-CCl_2 hybrids with pristine MWCNTs in which all the MWCNTs-CCl_2 hybrids, obtained from single site to tetra site PTC, were larger than the diameter of pristine MWCNTs (< 120 nm). The diameter of all the 4 types of MWCNTs-CCl_2 hybrids along with the pristine MWCNTs are given in Table 2. Hence, the gradual enhancement of the diameter in MWCNTs-CCl_2 hybrids is the reflection of the more functionalization and in turn confirms the availability of proportionate catalytic sites in PTCs. Hence, this result supported the HRTEM observation.

4. Conclusions

Two soluble MPTCs viz., BTEACM and TDMAPCB were developed, and they were characterized by FT-IR, ^{1}H-NMR, ^{13}C-NMR, TGA and EDS. The number catalytic sites (quaternary onium groups) generated in each catalysts were proved catalysis of CCl_2 functionalization on MWCNTs. That is, the two MPTCs were used as catalysts for sidewall functionalization of MWCNTs in dichlorocarbene addition, and compared their functionalization yield with commercially available single site PTC and tri-site PTC viz., BTEAC and TTEAMCM, respectively. The functionalization of CCl_2 on MWCNTs obtained from

the catalysis of newly developed MPTCs was established by the appearance of increased peak intensity of C-$Cl_{(str)}$ at 700 cm^{-1} and decreased peak intensity of C-$C_{(str)}$ at 1260 cm^{-1} in FTIR analysis. The gradual increase of I_D/I_G ratio from pristine MWCNTs (0.3) to MWCNT-CCl_2-4 hybrid (1.58) obtained from single site PTC to tetra site PTC in the Raman spectrum strongly supported the covalent functionalization of dichlorocarbene. The increased percentage weight loss of CCl_2 from single site PTC (0.9%) to tetra site PTC (12%) observed in TGA analysis further confirmed the sidewall functionalization of CCl_2 on MWCNTs. It was further supported by the observation of increased weight percentage of chlorine and decreased weight percentage of carbon in EDS results. Furthermore, the change of surface morphology from smooth to heterogeneous with white coverage observed in SEM and increased diameter of MWCNT-CCl_2 hybrids obtained from irrespective of MPTCs were confirmed by HRTEM, and AFM analyses. In a nutshell, the newly developed BTEACM and TDMAPCB catalysts are found to contain more active site (quaternary onium group) than commercially available single-site PTC. Among the all, the four catalysts produced more amount of CCl_2 functionalization on MWCNTs, the TDMAPCB catalyst produced more amount of CCl_2 yield on MWCNTs and thus it should contains more than three active site than other catalysts without much disrupting the electronic behavior of MWCNTs. Therefore, the tetra site PTC viz., TDMAPCB was proved to be an effective PTC for sidewall functionalization of MWCNTs in dichlorocarbene addition.

5. Acknowledgments

The authors are gratefully acknowledged the DST-Nanomission (DST-NSTI), New Delhi, Government of India, for financial assistance and Prof. C.N.R.Rao, Honorary President of Jawaharlal Nehru Centre for Advanced Scientific Research, Bangalore, India.

6. References

1. Iijima S. Helical microtubules of graphitic carbon. ***Nature.*** 1991, 354:56-58
2. Eder D. Carbon Nanotube−Inorganic Hybrids. ***Chem Rev.*** 2010, 110:1348-1385
3. Wu HXR, Tong XQ, Qiu HF, Yang YH and Lin RF. Functionalization of multiwalled carbon nanotubes with polystyrene under atom transfer radical polymerization conditions. ***Carbon***. 2007, 45:152-159
4. Wang S, Liang Z, Liu T, Wang B and Zhang C. Effective amino-functionalization of carbon nanotubes for reinforcing epoxy polymer composites. ***Nanotechnology***. 2006, 17:1551-1557
5. Tasis D, Tagmatarchis N, Bianco A and Prato M. Chemistry of carbon nanotubes. ***Chem Rev***. 2006, 106:1105-1136
6. Lin T, Bajpai V, Ji T and Dai LM. Chemistry of carbon nanotubes. ***Aust J Chem***. 2003, 56:635-651
7. Chen Y, Haddon RCS, Fang AMR, Eklund PCWH, Lee ECD and Grulke EA. Chemical attachment of organic functional groups to single-walled carbon nanotube material. ***J Mater. Res***. 1998, 13:2423-2431
8. Cumings J, Mickelson W and Zettl A. Simplified synthesis of double-wall carbon nanotubes. ***Solid State Commun***. 2003, 126:359-362
9. Ajayan PM and Ebbesen TW. Nanometre-size tubes of carbon. ***Rep Prog Phys***. 1997, 60:1025-1062
10. Dresselhaus MS, Dresselhaus G and Saito R. Physics of carbon nanotubes. ***Carbon***. 1995, 33:883-891
11. Rusca ID, Watari F and Uo M. Oxidation of multiwalled carbon nanotubes by nitric acid. ***Carbon***. 2005, 43:3124-3131
12. Hagen A and Talalaev GMV. Electronic structure and dynamics of optically excited single-wall carbon nanotubes. ***Appl Phys A***. 2004, 78:1137-1145

13. Xie J, Zhang N and Varadan VK. Functionalized carbon nanotubes in platinum decoration. ***Smart Mater Struct***. 2006, 15:S5-S8
14. Ugarte D, Stockli T and Bonard JM. Filling carbon nanotubes. ***Appl Phys A***. 1998, 67:101-105
15. Torre GDL, Blau W and Torres T. A survey on the functionalization of single-walled nanotubes. The chemical attachment of phthalocyanine moieties. ***Nanotechnology***. 2003, 14:765-771
16. Betbune DS, Klang CH and Vries MS. Cobalt-catalysed growth of carbon nanotubes with single-atomic-layer walls. ***Nature***. 1993, 363:605-607
17. Iijima S and Lchihashi T. Single-shell carbon nanotubes of 1-nm diameter. ***Nature***. 1993, 363:603-605
18. Hu H, Zhao R and Hamon MA. Sidewall functionalization of single-walled carbon nanotubes by addition of dichlorocarbene. ***J Am Chem Soc***. 2003, 125:14893-14900.
19. Chen J, Hamon MA and Hui YC. Solution properties of single-walled carbon nanotubes. ***Science***. 1998, 282:95-98
20. Kamaras K, Itkis ME and Hu H. Covalent Bond Formation to a Carbon Nanotube Metal. ***Science***. 2003, 301:1501
21. I,u X, Tian F and Zhang Q. The [2+1] Cycloadditions of dichlorocarbene, silylene, germylene, and oxycarbonylnitrene onto the sidewall of armchair (5,5) single-wall carbon nanotube. ***J Phys Chem B***. 2003,107:8388-8391
22. Bettinger HF. Addition of carbenes to the sidewalls of single-walled carbon nanotubes. Chemistry. 2006, 12:4372-4379
23. Jarrouse J. The influence of quaternary chemicals on the reaction of labile hydrogen compounds and chlorine-substituted derivatives. ***C R Hebd Seances Acad Sci Ser C***. 1951, 232:1424-1434
24. Freedman HH. Industrial applications of phase transfer catalysis (PTC): past, present and future. ***Pure Appl Chem***. 1986, 58:857-868
25. Starks CM and Liotta CL. Phase Transfer Catalysis, ***Academic Press***, NewYork, (Chapter 2), 1978
26. Dehmlow EV and Dehmlow SS. Phase Transfer Catalysis, ***Verlag***,Weinheim, 1993
27. Starks CM, Liotta CL and Halpern M. Phase Transfer Catalysis: Fundamentals, Applications and Industrial Perspectives, ***Chapman***, New York, 1994
28. Halpern M. Phase Transfer Catalysis Communications .1997, 3:33
29. Idoux JP, Wysocki R, Young S, Turcot J, Ohlman C and Leonard R. Polymer-Supported "Multi-Site" Phase Transfer. ***Catalysts Synth Commun***. 1983, 13:139-144
30. Balakrishnan T and Ford WT. The effect of polymer swelling on alkylation of phehylacetonitrile by polymer-supported phase transfer catalysis. ***Tetrahedron Lett***. 1981, 22:4377-4380
31. Balakrishnan T, Murugan E and Siva A. Synthesis and characterization of novel soluble multi-site phase transfer catalyst; its efficiency compared with single-site phase transfer catalyst in the alkylation of phenylacetonitrile as a model reaction. ***Appl Catal A: Gen***. 2004, 273:89-97
32. Murugan E and Siva A. Preparation of a novel soluble multi-site phase transfer catalyst and the kinetic study for the C-alkylation of α-pinene. ***J Mol Catal A Chem***. 2005, 235:220-229
33. Siva A and Murugan E. Synthesis and characterization of novel multi-site phase transfer catalyst and its catalytic efficiency for dichlorocarbene addition to citral. ***J Mol Catal A Chem***. 2005, 241:101-110
34. Murugan E and Siva A. Synthesis of asymmetric n-arylaziridine derivatives using a new chiral phase-transfer catalyst. ***Synthesis***. 2005, 2022-2028
35. Siva A and Murugan E. Syntheses of new dimeric-**C**inchona alkaloid as a chiral phase transfer catalysts for the alkylation of Schiff base. ***J Mol. Catal A Chem***. 2005, 241:111-117
36. Siva A and Murugan E. A new trimeric cinchona alkaloid as a chiral phase-transfer catalyst for the synthesis of asymmetric α-amino acids. ***Synthesis***. 2005, 2927-2933
37. Siva A and Murugan E. New trimeric **C**inchona alkaloid-based quaternary ammonium salts as efficient chiral phase transfer catalysts for enantioselective synthesis of α-amino acids. ***J Mol Catal. A Chem***. 2006, 248:1-9

38. Murugan E and Tamizharasu G. Synthesis and characterization of new soluble multisite phase transfer catalysts and their catalysis in free radical polymerization of methyl methacrylate aided by ultrasound - A kinetic study. ***Journal of Applied Polymer Science***. 2012, 125:263-273
39. Murugan E and Vimala G. Effective functionalization of multiwalled carbon nanotube with amphiphilic poly(propyleneimine) dendrimer carrying silver nanoparticles for better dispersability and antimicrobial activity. ***J Colloid and Interface Sci***. 2011, 357:354-365
40. Murugan E and Vimala G. Amphiphilic multiwalled carbon nanotube polymer hybrid with improved conductivity and dispersibility produced by functionalization with poly(vinylbenzyl)triethylammonium chloride. ***J Phys Chem C***. 2011, 115:19897-19909
41. Murugan E and Vimala G. Synthesis, characterization, and catalytic activity for hybrids of multi-walled carbon nanotube and amphiphilic poly(propyleneimine) dendrimers immobilized with silver and palladium nanoparticle. ***J Colloid and Interface Sci***. 2013, 96:101-111
42. Wang ML and Hsieh YM. Kinetic study of dichlorocyclopropanation of 4-vinyl-1-cyclohexene by a novel multisite phase transfer catalyst. ***J Mol Catal A Chem***. 2004, 210:59-68
43. Vajjiravel M and Umapathy MJ. Synthesis and characterization of multi-site phase transfer catalyst: application in radical polymerisation of acrylonitrile – a kinetic study. ***J Polym Res***. 2008, 15:27-36
44. Wu HS and Lee **CS.** Catalytic activity of quaternary ammonium poly(methylstyrene-**co**-styrene) resin in an organic solvent/alkaline solution. ***J Catal***. 2001,199:217-223
45. Zhou Z, Wang S, Lu L and Zhang Y. Functionalization of multi-wall carbon nanotubes with silane and its reinforcement on polypropylene composites. ***Comp Sci and Technol***. 2008, 68:1727-1733
46. Filho AGS, Jorio A, Samsonidze GG, Dresselhaus G, Saito R and Dresselhaus MS. Raman spectroscopy for probing chemically/physically induced phenomena in carbon nanotubes. ***Nanotechnology***. 2003, 14:1130-1139
47. Graupner R. Raman spectroscopy of covalently functionalized single-wall carbon nanotubes. ***J Raman Spectrosc***. 2007, 38:673-683
48. Dresselhaus MS and Eklund PC. Phonons in carbon nanotubes. ***Adv Phys***. 2000, 49:705-814